Journal of Solid State Chemistry **168,** 110–118 (2002)
doi:10.1006/jssc.2002.9697

Structure Evolution of Nanocrystalline CeO_2 Supported on Silica: Effect of Temperature and Atmosphere

L. Kępiński,[1] M. Wołcyrz, and M. Marchewka

Institute of Low Temperature and Structure Research, Polish Academy of Sciences, P.O. Box 1410, Wrocław 50-950, Poland

Received January 17, 2002; in revised form June 27, 2002; accepted July 15, 2002

Microstructure evolution of nanocrystalline CeO_2 supported on amorphous SiO_2 upon heat treatment in air or in hydrogen at 800–1100°C was studied by TEM, XRD, FTIR and Raman spectroscopy. Sintering of CeO_2 and SiO_2 with no interface reaction was observed up to 1100°C in air. In hydrogen, formation of various cerium silicates occurred depending on temperature and CeO_2:SiO_2 molar ratio. For CeO_2 content below $Ce_2Si_2O_7$ (disilicate) stoichiometry formation of a quasi-two-dimensional silicate was observed at 900–1050°C. Proposed structural formula of the silicate $Ce_6[Si_4O_{13}][SiO_4]_2$ and its lattice parameters: $a = 2.3422$, $b = 0.7196$, $c = 1.0082$ nm in $Pca2_1$ space group, indicate its close similarity to a group of $Ln_3[BSiO_6][SiO_4]$ borosilicates (Ln = La, Ce, Nd, Sm, Eu) and to I-type $La_2Si_2O_7$ disilicate. FTIR spectra of the silicate contain characteristic absorption band at 648 cm^{-1}, probably representing vibration of Si–O–Si bridge in $[Si_4O_{13}]$ group. © 2002 Elsevier Science (USA)

Key Words: **cerium silicate; $Ce_6[Si_4O_{13}][SiO_4]_2$, $Ce_2Si_2O_7$; CeO_2; ceria-silica reaction; TEM; FTIR.**

INTRODUCTION

Binary systems containing lanthanide oxide and SiO_2 are important in various fields of technology, including laser and optical fiber applications, microelectronics (as new high dielectric constant barriers) and catalysis. Among these, CeO_2–SiO_2 system plays a special role due to unusual properties of cerium oxide. CeO_2 with fluorite structure may exhibit large, reversible deviations from stoichiometry, CeO_{2-x} (x up to 0.3), and is used as oxygen storage medium in automotive exhaust catalysts. Moreover, Ce^{3+} ion is very efficient radiation absorber as well as emitter in blue/violet region.

In practical applications chemical reaction between nanocrystalline cerium oxide and SiO_2 support (or matrix) at elevated temperatures should be considered as possible cause of drastic modifications of both structure and chemical properties of the system. Analysis of CeO_2–SiO_2 phase diagram shows that six binary compounds (cerium silicates) may form at normal pressure: Ce_2SiO_5 (1), $Ce_{9.33}(SiO_4)_6O_2$ (2), two disilicates A- and G-$Ce_2Si_2O_7$ (1, 3) and recently reported $CeSiO_4$ with zircon structure (4). The last compound is the only cerium silicate containing Ce^{4+} ions. For lanthanum, two additional structure types H and I of disilicate were found recently (5, 6).

In the former paper (7) we reported on the amorphization of nanocrystalline CeO_2 supported on SiO_2 upon heating in H_2 above 600°C. We showed also, that Pd crystallites accelerate the process and serve as the nucleation centers for growth of crystalline $Ce_{9.33}(SiO_4)_6O_2$ silicate at 700°C. Recently, we studied luminescence properties of various nanocrystalline cerium silicates formed upon heating CeO_2–SiO_2 in H_2 at 900–1100°C (8). It appeared that new superficial cerium silicate with unknown structure stable at 900–1050°C exhibits strong emission in the violet/blue region (maximum around 400 nm) similar to that of tetragonal structures. On the contrary, hexagonal $Ce_{9.33}(SiO_4)_6O_2$ silicate showed very weak emission. In this work we present new results obtained for CeO_2–SiO_2 system by using various methods: XRD, TEM, IR and Raman spectroscopy. The main goal was to characterize fully the structure of the new superficial silicate phase found in (8) and give evidences that it represents a new polymorph of cerium disilicate, different from tetragonal A-$Ce_2Si_2O_7$.

EXPERIMENTAL

Sample Preparation

CeO_2/SiO_2 samples with various CeO_2 content were prepared by impregnation of SiO_2 gel powder with the appropriate amount of 20 wt% colloidal suspension of CeO_2 (Aldrich). Three SiO_2 supports were used: XOA-15 (Rhone-Poulenc) with surface area $S_a = 35\,m^2/g$ and

[1] To whom correspondence should be addressed. Fax: +48-71-344-10-29. E-mail: kepinski@int.pan.wroc.pl.

0022-4596/02 $35.00

average pore size 200 nm (denoted as R), Aerosil OX50 (Degussa), $S_a = 50\,m^2/g$ (D), and HS (Alfa), $S_a = 350\,m^2/g$ (A). The first support (R) contains some sodium (0.34 wt%), while the other two contain less than 0.001% of this element. Samples containing 30, 62, and 72 wt% CeO_2 described as 30CeSi(R or D), 62CeSi(D) and 72CeSi(A), respectively, were prepared. The last sample has stoichiometry close to that of $Ce_2Si_2O_7$ disilicate. The samples were dried overnight in air at 110°C then ground in a mortar. Heat treatment was performed in a tubular laboratory furnace in hydrogen flow or in air at 800–1100°C. Typical heating time was 3 h, though in some cases it was extended to 5 h.

Methods

Several complementary methods were used to characterize the structure of the samples. X-ray powder diffraction (XRD) patterns were obtained with Siemens D-5000 diffractometer (Ni-filtered Cu$K\alpha$ radiation). In some cases 30 wt% of corundum (α-Al_2O_3) powder (mean particle size $\sim$0.5 μm) was added to the samples as internal standard to enable determination of the true positions and width of reflections.

TEM and SEAD images were recorded with Philips CM20 SuperTwin microscope, which at 200 kV provides 0.25 nm resolution. Specimens for TEM were prepared by dispersing some powder sample in methanol and putting a droplet of the suspension on a copper microscope grid covered with perforated carbon.

FTIR and Raman spectra were acquired with Bruker IFS-88 spectrometer at a $2\,cm^{-1}$ resolution. Specimens for FTIR were prepared by mulling the powder sample with Nujol or with hexachloro-1,3-butadiene.

RESULTS

Heating in Air

Mean crystallite size of CeO_2 in "as-prepared" 30CeSi(R) sample was 6 nm (7). TEM revealed that CeO_2 particles were uniformly distributed over the support in "as-prepared" sample as well as in the samples heated in air up to 1050°C. With increasing temperature, we observed growth of a mean crystallite size of CeO_2 to 8, 14 and 40 nm at 800°C, 950°C and 1050°C, respectively. At 1050°C formation of some cristobalite was observed by XRD, but no evidence of growth of any cerium silicate could be found.

Raman spectra of 30CeSi(R) sample heated at 800°C and 1050°C revealed, in accordance with literature (9), sharpening of the F_{2g} peak from CeO_2 at $465\,cm^{-1}$ and its shift to higher wave number with increasing temperature of heating (and thus the size of CeO_2 particles). Interestingly, treatment of 30CeSi(R) sample in H_2 at 800°C caused disappearance of the F_{2g} line of CeO_2. This problem will be discussed later in the paper.

Heating in Hydrogen

XRD

Figure 1 shows XRD patterns of 30CeSi(R) sample heated in H_2 at 800°C (a), 900°C (b), 1050°C (c) and 1100°C (d). Patterns of the 30CeSi(D) sample prepared from Na-free SiO_2(D) were very similar and are not shown. In Figs. 1a–c, peaks of a corundum standard are marked with dots. For comparison, in Fig. 1a XRD pattern of 30CeSi(R) sample heated in air at 800°C is shown. It appears that heating in H_2 at 800°C caused complete disappearance of CeO_2 reflections. At 900°C broad reflections of a new phase became visible at ca. 27°, 28.6°, and 30.5°. Increase of temperature up to 1050°C resulted only in some sharpening of the reflections. The observed pattern could not be assigned to any known compound occurring in the CeO_2–SiO_2 system. At 1100°C drastic changes occurred, involving crystallization of SiO_2 into cristobalite (reflections marked with squares) and

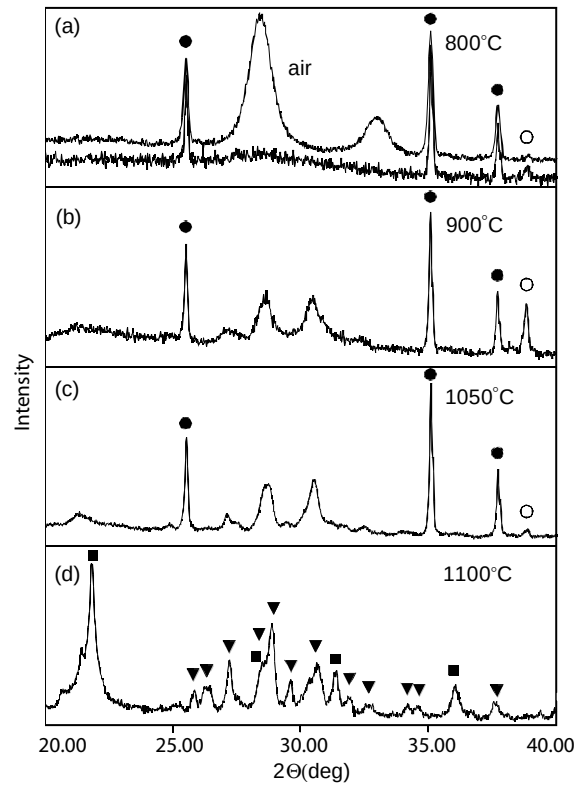

FIG. 1. XRD patterns of 30CeSi(R) sample heated in H_2 at 800°C (a), 900°C (b), 1050°C (c) and 1100°C (d). In (a) pattern of 30CeSi(R) sample heated in air at 800°C is included. —corundum standard, ■—cristobalite, ▼—A-$Ce_2Si_2O_7$, ○—sample holder.

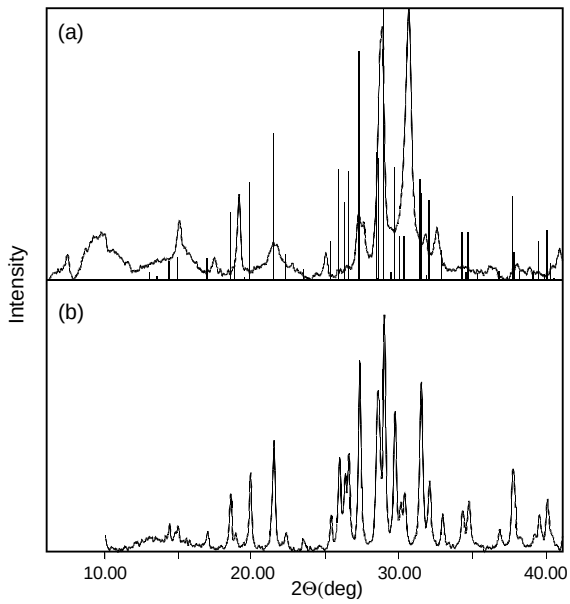

FIG. 2. XRD patterns of 62CeSi(D) heated at 1000°C (a) and 72CeSi(A) heated at 1100°C (b).

transformation of the new silicate phase into tetragonal A-$Ce_2Si_2O_7$ (reflections marked with triangles).

Figure 2 depicts XRD patterns of the samples with higher amount of CeO_2: 62CeSi(D) heated at 1000°C (a) and 72CeSi(A) heated at 1100°C (b). Pattern (a) is in fact the better developed pattern of the undefined silicate phase (cf. Fig. 1) while pattern (b) fits very well the known pattern of tetragonal A-$Ce_2Si_2O_7$ disilicate (1). Since we could not find in literature crystal structure data (atomic positions) of tetragonal A-$Ce_2Si_2O_7$, we performed the Rietveld refinement procedure (10) using the data of lanthanum silicate analogue (11) as a starting point. The results are given in Table 1. Additionally, schematic XRD pattern calculated using these data is included in Fig. 2a which shows the differences between the undefined cerium silicate and A-$Ce_2Si_2O_7$.

TABLE 1
Results of the Rietveld Refinement of A-$Ce_2Si_2O_7$ Silicate

Atom	Wyckoff position	x	y	z	B (Å^2)
Ce1	4(*a*)	0.7639(6)	0.2984(5)	0.0000(2)	1.5(2)
Ce2	4(*a*)	0.5211(5)	0.1689(5)	0.1476(3)	1.8(2)
Ce3	4(*a*)	0.3349(6)	0.9215(4)	0.0003(2)	1.6(2)
Ce4	4(*a*)	0.1150(5)	0.7722(6)	0.1403(2)	1.5(2)
Si1	4(*a*)	0.861(2)	0.766(2)	0.013(1)	1.0(4)
Si2	4(*a*)	0.602(2)	0.693(2)	0.113(1)	1.1(4)
Si3	4(*a*)	0.249(2)	0.382(2)	0.022(1)	2.1(5)
Si4	4(*a*)	0.046(2)	0.277(2)	0.124(1)	2.1(6)
O1	4(*a*)	0.883(5)	0.636(5)	−0.021(1)	1.5
O2	4(*a*)	0.726(5)	0.929(5)	−0.008(1)	1.5
O3	4(*a*)	0.048(5)	0.819(5)	0.045(1)	1.5
O4	4(*a*)	0.701(4)	0.643(4)	0.061(1)	1.5
O5	4(*a*)	0.474(5)	0.544(4)	0.138(1)	1.5
O6	4(*a*)	0.425(5)	0.846(5)	0.102(1)	1.5
O7	4(*a*)	0.733(4)	0.813(4)	0.149(1)	1.5
O8	4(*a*)	0.329(5)	0.573(4)	−0.011(1)	1.5
O9	4(*a*)	0.433(5)	0.237(4)	0.042(1)	1.5
O10	4(*a*)	0.119(5)	0.264(4)	−0.017(1)	1.5
O11	4(*a*)	0.126(5)	0.429(4)	0.071(2)	1.5
O12	4(*a*)	−0.023(5)	0.467(4)	0.165(2)	1.5
O13	4(*a*)	0.136(4)	0.135(5)	0.150(2)	1.5
O14	4(*a*)	−0.191(4)	0.230(5)	0.097(1)	1.5

Note. The temperature factors for O atoms were fixed to the values of 1.5 Å^2. For all the refined parameters standard deviations are given in parentheses. Space group: $P4_1$ (No. 76), lattice parameters: $a = 0.6798(1)$ nm, $c = 2.4726(1)$ nm, $Z = 8$, profile discrepancy factors: $R_p = 2.67\%$, $R_{wp} = 3.43\%$.

FTIR Spectroscopy

Figure 3 shows FTIR spectra (MIR and FIR) of 30CeSi(R) sample heated in H_2 at 800°C, 950°C and 1100°C (positions and intensities of absorption bands are given in Table 2). The spectrum of the sample heated at 800°C is very similar to that of amorphous SiO_2 with additional broad bands at 530–600 and 840–1000 cm^{-1} (cf. Table 2). In Table 2 bands that could originate from SiO_2 (amorphous or cristobalite) are given in italics. At 950°C new absorption bands occurred at 543, 648, 680, 827, 912, 943 and 977 cm^{-1}. At 1100°C many sharp bands appeared (cf. Table 2), some of them at 386, 621, 795 and 1207 cm^{-1} originating from cristobalite. In Fig. 4, FTIR spectra of the samples with higher CeO_2 content are shown: 62CeSi(D) heated at 1000°C and 72CeSi(A) heated at 1100°C (A-$Ce_2Si_2O_7$). To enable observation of IR bands eventually obscured by Nujol band at 721 cm^{-1}, we also acquired the spectra of the samples dispersed in hexachloro-1,3-butadiene (the results are included as insets in Fig. 4). It appears that for the new phase there are three weak bands in this spectral range but none for A-$Ce_2Si_2O_7$ (cf. Table 2). As for XRD, spectrum of 62CeSi(D) sample contains better developed bands seen already in 30CeSi(R) sample heated at 950°C. FTIR spectrum of 72CeSi(A) agrees well with those of other A-type lanthanide disilicates published by Lazarov (12). The general conclusion is that although the spectrum of the new silicate phase bears some resemblance to that of A-$Ce_2Si_2O_7$ disilicate, there are important differences in both the number and positions of the absorption bands.

Unfortunately, despite numerous attempts and using both classic (514 nm) as well as Fourier (1064 nm) instruments, very strong fluorescence precluded obtaining satisfactory Raman spectra of the CeO_2/SiO_2 samples heated in hydrogen.

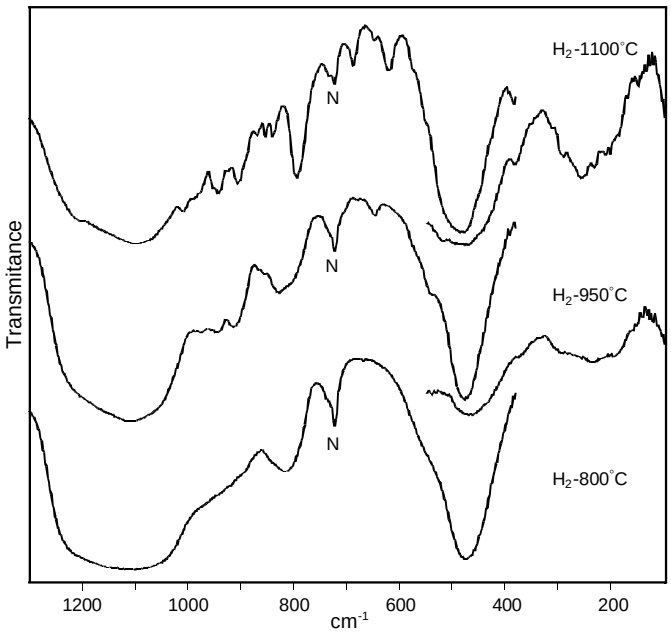

FIG. 3. FTIR spectra of 30CeSi(R) sample heated in H_2 at 800°C, 950°C and 1100°C. N—Nujol.

TEM

TEM micrographs of 30CeSi(R) sample heated at 800°C (not shown) revealed no crystalline phase present in accordance with XRD. At 900°C new crystalline phase is formed (Fig. 5a). It is clearly seen that the new phase covers substantial area of SiO_2 support as thin, quasi-two-dimensional layer. At 1000°C this phase undergoes some sintering and flat irregular particles form. Simultaneously, sintering of SiO_2 also occurs. Dramatic change in the particle morphology occurred upon heating at 1100°C (Fig. 5b). Crystallization of SiO_2 into large cristobalite particles and formation of well-developed, rod-like silicate crystallites with size of 20–200 nm took place. Most abundant rod-like crystallites have been identified as low temperature, tetragonal A-$Ce_2Si_2O_7$. The sample however, contains, also small amount of other phases: irregular oblate crystallites identified as monoclinic G-$Ce_2Si_2O_7$ and small, flat crystallites of the new phase.

Determination of the Crystal Structure of the New Cerium Silicate

The superficial (quasi-two-dimensional) nature of the new cerium silicate results in rather weak and broad XRD reflections, making the structure determination very difficult. We used, therefore, SAED and HRTEM to obtain a rough estimation of the unit-cell parameters. In Fig. 6, SEAD patterns of a crystallite of the new phase in three different orientations are presented. By using a special software WINREKS (13) the patterns were combined together to form a portion of the reciprocal lattice. Observation of various projections of the lattice during its rotation enabled us to find out low index sections and thus probable symmetry and dimensions of the unit cell (orthorhombic with cell parameters 1.00, 0.72 and 2.35 nm). Using such unit cell we were able to index most of SAED patterns as well as FFT patterns obtained from HRTEM images of various crystallites of the new phase. In particular, zone axes in Fig. 6 could be indexed as $[\bar{1}00]$, $[\bar{1}10]$ and $[\bar{2}10]$, respectively. Interzone angles measured from the goniometer settings and calculated for the assumed structure agreed to within 2°. The radii of the first Laue zone measured from CBED patterns and calculated for the assumed structure also agreed to within 5%. In experimental SAED patterns some disorder in direction perpendicular to the (001) planes and the effect of strong bending are visible. The effect of bending is easily explained by the superficial nature of the new phase, which spreads over irregular SiO_2 grains. Experimental SAED patterns in Fig. 6 are compared with the corresponding patterns calculated with HREM module of Cerius[2] package for the model of the crystal structure obtained by the Rietveld refinement (see below).

A literature search revealed that there is a group of lanthanide borosilicates with general formula $Ln_3[BSiO_6][SiO_4]$, where Ln = Nd (14), Sm (15), Eu (16), Ce (17) or La (18) which have orthorhombic structure, *Pbca* space group and unit cell parameters $a = 0.9900, b = 0.7203, c = 2.3292$ nm for Ce (17), very similar to that of our new silicate. XRD diagram calculated from single crystal data for $Ce_3[BSiO_6][SiO_4]$ (17) also showed distinct similarity with our experimental diagram. We used therefore the structure of cerium borosilicate (17) as an initial model of the new silicate. Since there was no boron in our compound we substituted it with silicon and to compensate the electric charge, one O^{-2} ion was introduced between two Si_2O_6 groups. Fig. 7 shows fragment of the crystal structure of $Ce_3[BSiO_6][SiO_4]$ before (a) and after the transformation (b). The positions of Si and O atoms in (b) were optimized by using the DLS module of Cerius[2] package. Since the number of additional O atoms is only half of that of Si, the symmetry of the structure had to be lowered from *Pbca* to its subgroup $P2_1ca$ and then, to be consistent with the standard setting in the International Tables for Crystallography, we had to transform the unit cell to $Pca2_1$. The overall formula thus becomes: $Ce_6[Si_4O_{13}][SiO_4]_2$ (stoichiometry of the compound is the same as disilicates, i.e., $Ln_2O_3 + 2SiO_2$) and the structure contains $[Si_4O_{13}]$ groups of four $[SiO_4]$ tetrahedra shearing corners and additionally isolated $[SiO_4]$ tetrahedra. Such a model has been used as a starting point in the Rietveld refinement procedure. The results are given in Figs. 8 and 9 and in Table 3. When comparing calculated diagram with

TABLE 2

Wavenumbers (cm^{-1}) and Relative Intensities[a] of the Bands Observed in the Powder FTIR Spectra of CeO_2/SiO_2 Samples Heated in Hydrogen

30CeSi(R)			62CeSi(D)	72CeSi(A)
H_2-800	H_2-950	H_2-1100	H_2-1000	H_2-1100
		1198vssh		
1188vssh	*1185vssh*			
1109vsb	*1107vsb*	*1098vsb*	*1099vs*	
			1047vs	
			1031vs	1035vs
			1014vs	
		1009vs		1003vs
		987s		985vs
977ssh	977s	977s	974vs	976vs
		952s		951vs
	944s	942s	944vs	941vs
		925s		924vs
	914s	907s	907vs	899vs
		890ssh		887vs
		870m	869vs	869vs
		854m	857vs	852vs
		839m	836vs	838vs
	828m			
814m				
	807msh	*794s*		
			770w	
			731w	
	703vw		703w	
		688w	685w	687vs
	646vw	648vw	648w	
		620w		
		572w	576msh	575vs
534msh	540msh	548msh	541s	553vs
				528vs
		518vssh	515s	
				496vs
			482vs	
475vs	*478vs*	*480vs*		*473vs*
				450vs
	436msh		439m	
				426s
	377w	*384w*		*387m*
				370m
				352m
				343m
		312w		316s
	294	*291w*	*288w*	*293s*
				271vs
		258w		259vs
			245m	251vs
	237w	232w		232vs
				212vs
	195w		199m	
		188w		185vs
				169s
				156m
				147s

TABLE 2 —*Continued*

30CeSi(R)			62CeSi(D)	72CeSi(A)
H_2-800	H_2-950	H_2-1100	H_2-1000	H_2-1100
				136s
				112vw
				102m
				93w

Note. Bands in italics may originate from SiO_2.

[a] Abbreviations: s—strong, w—weak, v—very, sh—shoulder, b—broad, m—medium.

an experimental one it appears that some reflections in the latter are much wider than an average. These reflections, namely 411, 412, 811 and 1013, have their diffraction vectors close to [111] direction. It may indicate that crystallites of the new phase grow in preferential manner such that [111] is perpendicular to the surface of SiO_2 support. An alternative explanation could be the disorder along [111] direction. The crystal structure obtained by Rietveld refinement was then used in calculations of simulated HRTEM images and SAED patterns.

In Fig. 10, experimental HRTEM image of a crystallite of the new phase in [02$\bar{1}$] orientation is compared with a simulated image (inset). Agreement is reasonably good, further confirming the applicability of the assumed model. It should be remembered, however, that due to limited resolution of our microscope only positions of Ce atomic columns can be discerned in the image (white dots).

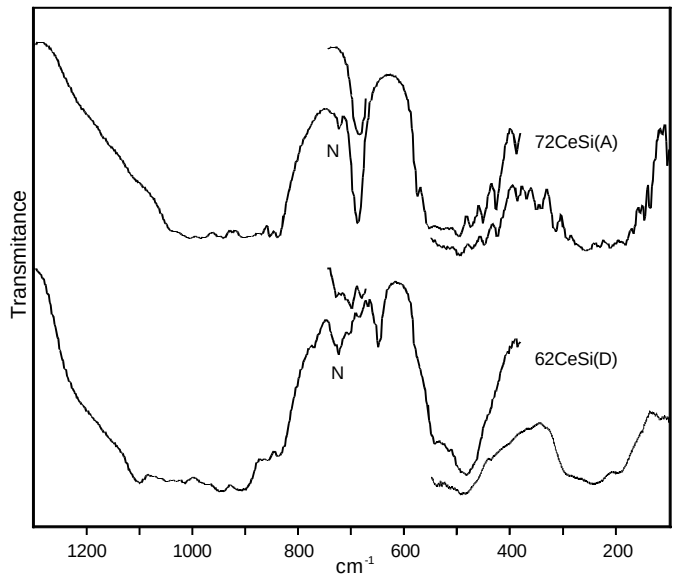

FIG. 4. FTIR spectrum of 62CeSi(D) heated in H_2 at 1000°C compared with spectrum of 72CeSi(A) heated in H_2 at 1100°C (A-$Ce_2Si_2O_7$). Spectra of the samples prepared in hexachloro-1,3-butadiene are included as insets.

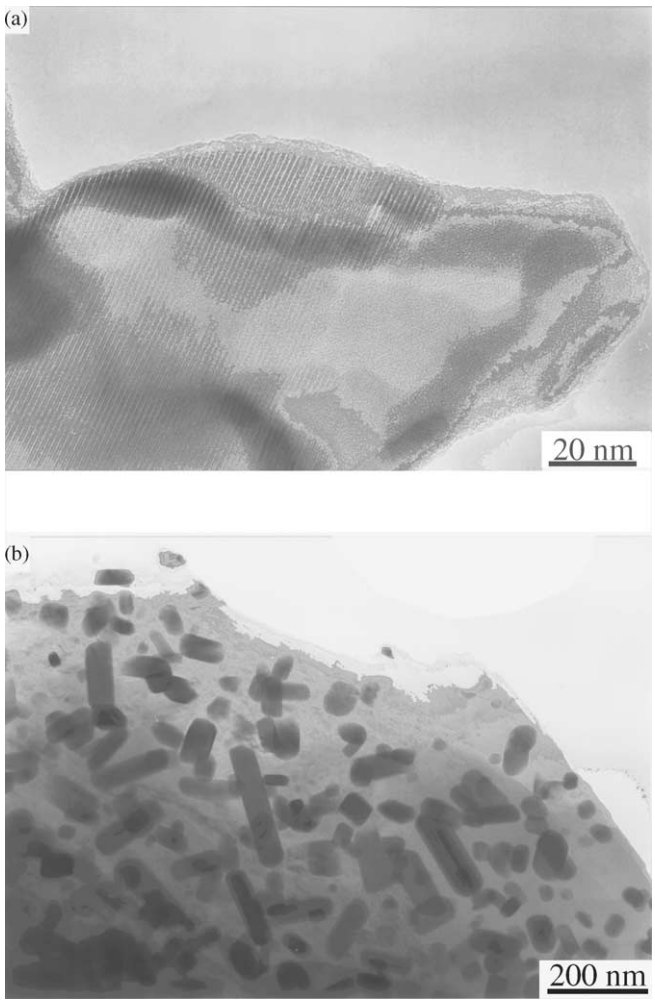

FIG. 5. TEM micrographs of 30CeSi(R) sample heated in H_2 at 900°C (a) and at 1100°C (b).

DISCUSSION

Heating of 30CeSi(R) sample in air up to 1050°C caused only sintering of CeO_2 and SiO_2 (with its partial crystallization to cristobalite) without formation of any new phase. It corresponds to results of van Hal and Hintzen (1), who observed formation of $Ce_2Si_2O_7$ silicates in CeO_2–SiO_2 system in air only above 1400°C. $CeSiO_4$ silicate (containing Ce^{4+}), reported recently by Skakle *et al.* (4), was obtained at 1000°C in hydrothermal conditions in the presence of CaO. Appearance of cristobalite in 30CeSi(R) sample at unusually low temperature of 1050°C (at 950°C for bare SiO_2(R) support), is obviously connected with the presence of Na (0.35 wt%) in the SiO_2(R) support. Takeuchi *et al.* (19) showed that addition of 5 wt% Na_2CO_3 to SiO_2 gel lowers the onset temperature of cristobalite formation from 1200°C to 650°C.

Results of heating in hydrogen are more interesting. Observation and tentative description of the structure of the new quasi-two-dimensional Ce silicate with complex $Ce_6[Si_4O_{13}][SiO_4]_2$ structure formed at 900°C is the most important result of our work. Taking into account the rather poor quality of the Rietveld refinement fit and limited resolution of HRTEM images, we must say that the structure proposed in this paper for the new cerium silicate phase is more or less hypothetical. In particular, the lengths of Si–O bonds are rather unusual since the bridge Si–O bonds (within Si–O–Si chain) are longer than that of terminal Si–O bonds. In most sorosilicates, except $Sm[Si_2O_7]_3$, $Nd_2[Si_2O_7]$, $Sc_2[Si_2O_7]$, and $Ba_3Nd_6[Si_2O_7]_2O_{12}$, the opposite is true (20). The Si–O–Si angles in the proposed structure (139°, 146°, 140°) are close to 140° where minimum energy of Si_2O_7 group occurs, and which is the mean value for all sorosilicates (20).

The silicate grows only in excess of SiO_2 and apparently is stable only as a two-dimensional phase. Similar

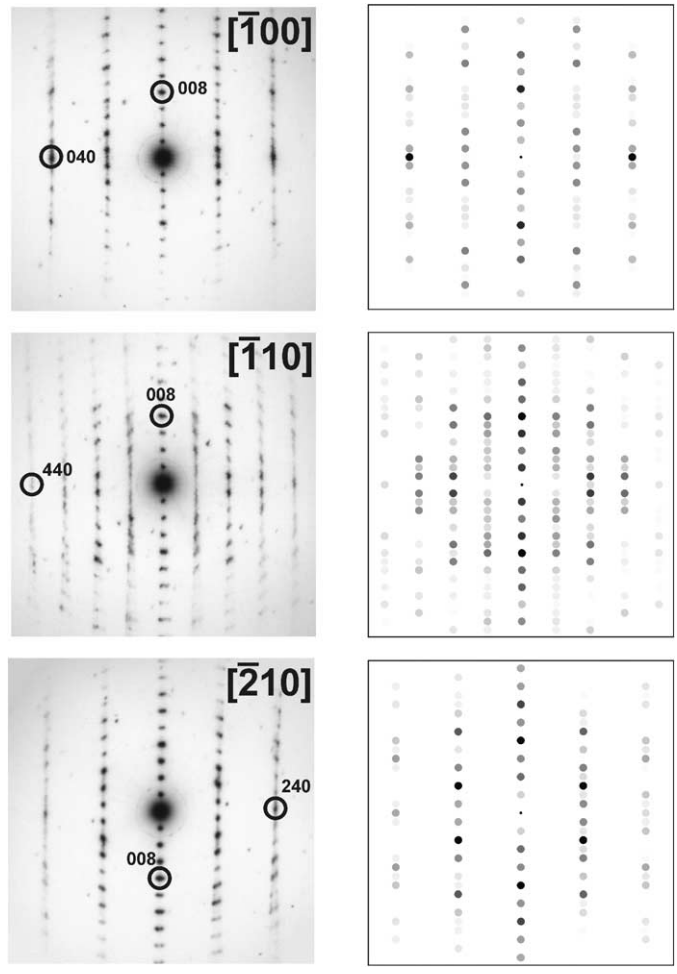

FIG. 6. Experimental and calculated SEAD patterns of a crystallite of the new phase in three different orientations.

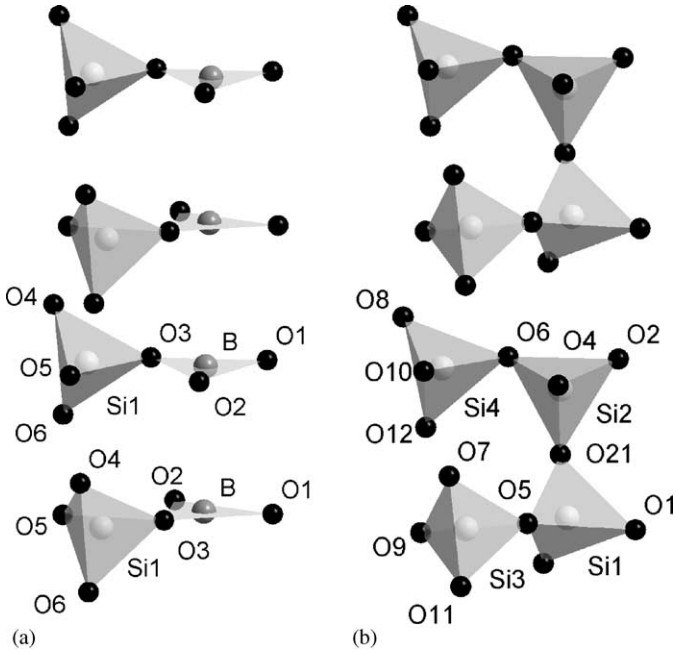

FIG. 7. The comparison of the columns of the oxygen polyhedra in $Ce_3[BSiO_6][SiO_4]$ (a) and $Ce_6[Si_4O_{13}][SiO_4]_2$ (b) structures. Addition of O21 atoms and substitution of Si1 and Si2 for B allow to build the starting model for the crystal structure refinement of $Ce_6[Si_4O_{13}][SiO_4]_2$.

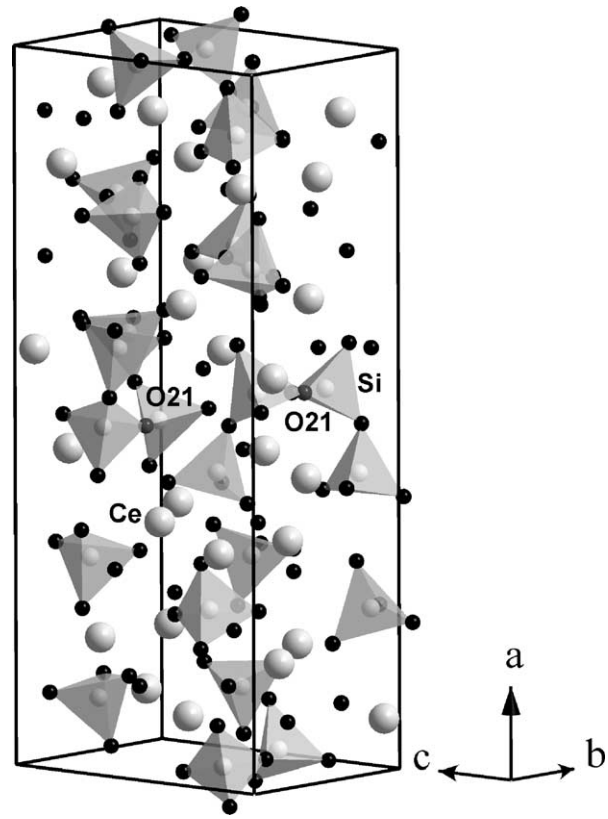

FIG. 9. Unit cell of the $Ce_6[Si_4O_{13}][SiO_4]_2$. Additional O21 oxygens connecting $[Si_2O_7]$ dihedra into $[Si_4O_{13}]$ groups are marked.

behaviour was observed for yttrium disilicate described as *y*-form (21). In their original work (21) Ito and Johnson stated: "…a single *y*-phase is stable only at a chemical composition richer in SiO_2 than that of $Y_2Si_2O_7$ at temperatures between 900°C and 1050°C in air…". Three-dimensional, bulk single crystals of *y*-$Y_2Si_2O_7$ were obtained only with addition of 4% thorium oxide (22). In the case of cerium silicate studied in this work addition of boron apparently is able to stabilize the structure in three

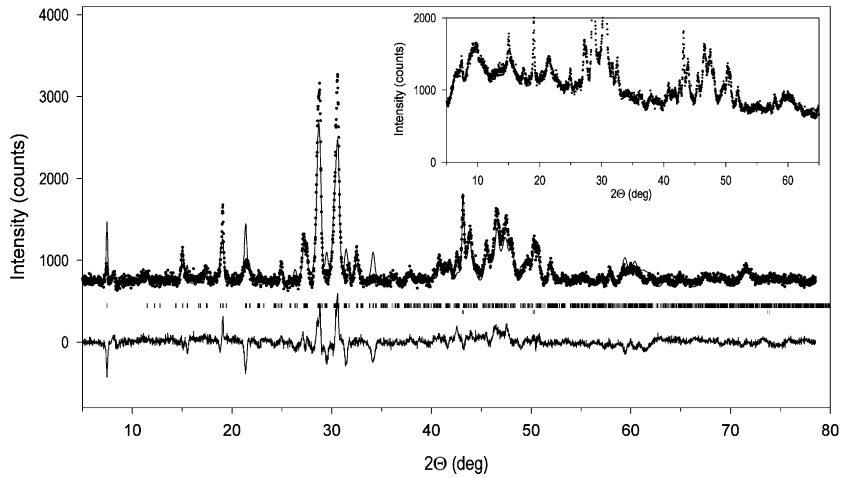

FIG. 8. Graphical representation of the crystal structure Rietveld refinement procedure for $Ce_6[Si_4O_{13}][SiO_4]_2$. Full circles represent experimental data, solid line—calculated diagram. Below, sticks representing peak positions for the silicate (upper row) and copper coming from the sample holder (lower row) and differential diagrams are plotted. As an inset the "as-measured" diagram of the silicate is shown with the complex background clearly seen.

TABLE 3
Results of the Rietveld Refinement of the New $Ce_6[Si_4O_{13}][SiO_4]_2$ Silicate

Atom	Wyckoff position	x	y	z	B (Å^2)
Ce1	4(*a*)	0.5741(7)	0.6208(35)	0.5086(20)	1.00
Ce2	4(*a*)	0.4259(7)	0.8792(39)	0.4914(19)	1.00
Ce3	4(*a*)	0.6619(7)	0.6053(38)	0.1353(19)	1.00
Ce4	4(*a*)	0.3381(6)	0.8947(41)	0.8647(18)	1.00
Ce5	4(*a*)	0.8180(7)	0.3421(41)	0.2581(20)	1.00
Ce6	4(*a*)	0.1820(8)	0.1579(40)	0.7419(20)	1.00
Si1	4(*a*)	0.0313	0.5703	0.2479	1.00
Si2	4(*a*)	0.9758	0.8552	0.7199	1.00
Si3	4(*a*)	0.9171	0.6029	0.3966	1.00
Si4	4(*a*)	0.0912	0.9164	0.6164	1.00
Si5	4(*a*)	0.7236	0.5935	0.4363	1.00
Si6	4(*a*)	0.2764	0.9065	0.5637	1.00
O1	4(*a*)	0.0979	0.6048	0.3075	1.00
O2	4(*a*)	0.9136	0.9555	0.6808	1.00
O3	4(*a*)	0.0156	0.7271	0.1325	1.00
O4	4(*a*)	0.9884	0.8752	0.8741	1.00
O5	4(*a*)	0.9830	0.5852	0.3552	1.00
O6	4(*a*)	0.0240	0.9567	0.6297	1.00
O7	4(*a*)	0.8929	0.4250	0.4845	1.00
O8	4(*a*)	0.1260	0.0810	0.5296	1.00
O9	4(*a*)	0.8802	0.6237	0.2548	1.00
O10	4(*a*)	0.1201	0.9125	0.7671	1.00
O11	4(*a*)	0.9065	0.7908	0.4862	1.00
O12	4(*a*)	0.1020	0.7159	0.5455	1.00
O13	4(*a*)	0.7098	0.5624	0.5990	1.00
O14	4(*a*)	0.2907	0.9410	0.4077	1.00
O15	4(*a*)	0.7914	0.6678	0.4236	1.00
O16	4(*a*)	0.2086	0.8322	0.5764	1.00
O17	4(*a*)	0.6775	0.7529	0.3741	1.00
O18	4(*a*)	0.3225	0.7471	0.6259	1.00
O19	4(*a*)	0.7180	0.3916	0.3512	1.00
O20	4(*a*)	0.2820	0.1084	0.6488	1.00
O21	4(*a*)	0.9715	0.6362	0.6731	1.00

Note. Space group: $Pca2_1$ (No. 29), Lattice parameters: $a = 2.3422(3)$ nm, $b = 0.7196(1)$ nm, $c = 1.0082(1)$ nm, $Z = 4$.
Profile discrepancy factors: $R_p = 6.56\%$, $R_{wp} = 8.92\%$.

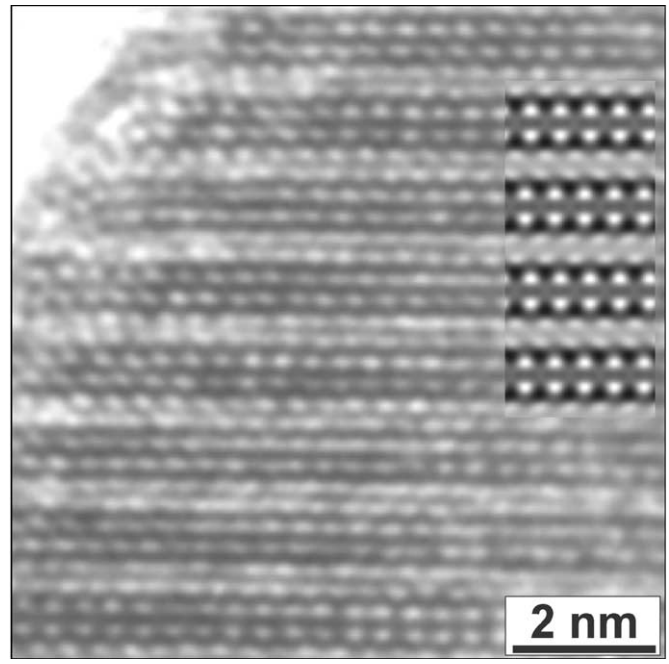

FIG. 10. Experimental HRTEM image and simulated image (inset) of a crystallite of the new phase in [02$\bar{1}$] orientation.

dimensions (5). There are two possible factors stabilizing the $Ce_6[Si_4O_{13}][SiO_4]_2$ as a quasi-two-dimensional phase: interaction with the SiO_2 support and the surface energy. Examples of the latter are Al_2O_3 and ZrO_2, which in highly dispersed state assume crystal structures different from that considered as thermodynamically stable (23,24).

A characteristic feature of the new silicate is its FTIR spectrum, which contains several bands in the 600–750 cm^{-1} region including a strong band at 650 cm^{-1} (cf. Figs. 3 and 4 and Table 2). Interestingly, we have found that quite similar absorption band at ca. 650 cm^{-1} occurs in IR spectrum of y-$Y_2Si_2O_7$ (not shown). In (25), the authors found a strong band at 650 cm^{-1} in the IR spectrum of silver silicate, but attributed it to unknown contamination. We propose that the band at 650 cm^{-1} may originate from a special arrangement of SiO_4 tetrahedra (possibly a group of four units sharing one corner). There are few known silicates having similar $[Si_4O_{13}]$ groups: $Ag_{18}[Si_4O_{13}][SiO_4]$ (26) of monoclinic $C\ 2/m$ structure, $Ag_{10}[Si_4O_{13}]$, triclinic (27) and $Nd_4Sc_2[Si_4O_{13}]$ (28). Unfortunately, we could not find IR spectra of those compounds to verify our hypothesis.

FTIR spectra of A-type $Ln_2Si_2O_7$ disilicates (Ln = Nd, Sm, Eu) were published by Lazarov (12) and are similar to the spectrum of A-$Ce_2Si_2O_7$ reported in this work. An interesting point is, however, FIR spectrum of A-$Ce_2Si_2O_7$ silicate (Fig. 4), which is extremely complex. The large number of bands in the FIR region is probably a consequence of large size and lack of a center of symmetry of the unit cell ($P4_1$ space group). For the new cerium silicate the number of bands is smaller, which is consistent with the existence of the center of symmetry of the unit cell ($Pca2_1$ space group). It is a pity that we could not obtain acceptable Raman spectra of cerium silicates, as those could give important information on the configuration of $[SiO_4]$ tetrahedra. In particular position of stretching terminal Si–O bond vibration gives information on the number of the bridging Si–O–Si bonds (29).

Recently, Müller-Bunz and Schleid (30) reported single-crystal structure data for the new lanthanum silicate with $La_6[Si_4O_{13}][SiO_4]_2$ formula (I-type $La_2Si_2O_7$) mentioned in (6). The unit cell ($P2_1/c$; $a = 0.7273, b = 2.3572$, $c = 1.0129$ nm, $\beta = 90.338^\circ, Z = 12$) is similar to that reported in this paper, however, the symmetry is lower. We therefore performed the Rietveld refinement procedure for our superficial cerium silicate phase using the structure

model given in (30). The results were comparable to ours. However, in both cases we observed similar discrepancies between measured and calculated diffraction patterns. It seems possible therefore that yet another structure model is necessary to describe properly the crystal structure of the superficial cerium silicate studied in this work.

ACKNOWLEDGMENTS

The authors thank Mrs. L. Krajczyk and Mrs. Z. Mazurkiewicz for valuable help with preparation of the samples and TEM work. Special thanks are due to Dr. M. Drozd for the acquisition of the Raman spectra of the samples heated in air. Calculations using Cerius^2 package were performed on the computers of the Wrocław Center of Networking and Supercomputing.

REFERENCES

1. H. A. M. van Hal and H. T. Hintzen, *J. Alloys Compd.* **179,** 77–85 (1992).
2. E. L. Belokoneva, T. L. Petrova, M. A. Simonov, and V. A. Belov, *Kristallografiya* **17,** 490–493 (1972).
3. A. C. Tas and M. Akinc, *J. Am. Ceram. Soc.* **77,** 2968–2970 (1994).
4. J. M. S. Skakle, C. L. Dickson, and F. P. Glaser, *Powder Diffraction* **15,** 234–238 (2000).
5. H. Müller-Bunz and T. Schleid, *Z. Anorg. Allg. Chem.* **626,** 2549–2556 (2000).
6. A. Müller-Bunz and T. Schleid, *Z. Kristallogr.* Suppl. **16,** 95–95 (1999).
7. L. Kępiński and M. Wołcyrz, *J. Solid State Chem.* **131,** 121–130 (1997).
8. L. Kępiński, D. Hreniak, and W. Stręk, *J. Alloys Compd.* **341,** 203–207 (2002).
9. G. W. Graham, W. H. Weber, C. R. Peters, and R. Usmen, *J. Catal.* **130,** 310–313 (1991).
10. R. A. Young, A. Sakthivel, T. S. Moss, and C. O. Paria-Santos, *J. Appl. Crystallogr.* **28,** 366–367 (1995).
11. A. M. Dago, D. Yu. Pushcharovskii, E. E. Strelkova, E. A. Pobedimskaya, and N. V. Belov, *Dokl. Akad. Nauk SSSR* **252,** 1117–1121 (1980).
12. A. Lazarov, "Kolebatelnyje Spektri i Stroenie Silikatov." Nauka, Leningrad, 1968.
13. M. Wołcyrz and M. Andruszkiewicz, *in* "Electron Crystallography" (D. L. Dorset, S. Hovmöller, and X. Zou, Eds.), p. 427. Kluwer Academic Publishers, Dordrecht, 1997.
14. H. Müller-Bunz and T. Schleid, *Z. Kristallogr.* Suppl. **15,** 48–48 (1998).
15. L. Chi, H. Chen, S. Deng, H. Zhuang, and J. Huang, *J. Alloys Compd.* **242,** 1 (1996).
16. L. Chi, H. Chen, S. Deng, H. Zhuang, and J. Huang, *Acta Crystallogr. C* **52,** 2385 (1996).
17. H. Müller-Bunz and T. Schleid, *Z. Anorg. Allg. Chem.* **627,** 1436 (2001).
18. E. V. Shvanski, N. I. Leonyuk, G. Bocelli, and L. Righi, *J. Solid State Chem.* **154,** 312–316 (2000).
19. N. Takeuchi, S. Yamane, S. Ishida, and H. Nanri, *J. Non-Cryst. Solids* **203,** 369–374 (1996).
20. F. Liebau, "Structural Chemistry of Silicates." Springer-Verlag, Berlin, 1985.
21. J. Ito and H. Johnson, *Am. Mineral.* **53,** 1940–1952 (1968).
22. N. Batalieva and Yu. A. Piatenko, *Kristallografiya.* **16,** 905–910 (1971).
23. J. M. McHale, A. Auroux, A. J. Perrotta, and A. Navrotsky, *Science* **277,** 788 (1997).
24. T. Yamaguchi, *Catal. Today* **20,** 199 (1994).
25. A. Möller and P. Amann, *Z. Anorg. Allg. Chem.* **627,** 172–179 (2001).
26. K. Heidebrecht and M. Jansen, *Z. Anorg. Allg. Chem.* **597,** 79–86 (2001).
27. M. Jansen and H. L. Keller, *Anorg. Chem.* **91,** 500–506 (1979).
28. B. A. Maksimov, O. K. Melnikov, T. A. Zhdanova, V. V. Ilyukin, and N. V. Belov, *Dokl. Akad. Nauk SSSR* **251,** 98–102 (1980).
29. P. McMillan, *Am. Minerol.* **69,** 622 (1984).
30. H. Müller-Bunz and T. Schleid, *Z. Anorg. Allg. Chem.* **628,** 564–569 (2002).